Scientific Research Publishing

Advances in Materials Physics and Chemistry, 2017, 7, 277-293
http://www.scirp.org/journal/ampc
ISSN Online: 2162-5328
ISSN Print: 2162-531X

Investigation of Niobium (Nb) Substitution on Structural and Superconducting Properties of (Bi, Pb)-Based Superconductors

Reza Asghari[1,2], Hasan Sedghi[1], Leyla Çolakerol Arsalan[3], Hamid Naghshara[2]

[1]Department of Physics, Superconductivity Research Center, Urmia University, Urmia, Iran
[2]Department of Solid state and Electronic, Faculty of Physics, Tabriz University, Tabriz, Iran
[3]Department of Physics, Gebze Technical University, Gebze, Turkey
Email: r.asghari@tabrizu.ac.ir

How to cite this paper: Asghari, R., Sedghi, H., Arsalan, L.Ç. and Naghshara, H. (2017) Investigation of Niobium (Nb) Substitution on Structural and Superconducting Properties of (Bi, Pb)-Based Superconductors. *Advances in Materials Physics and Chemistry*, **7**, 277-293.
https://doi.org/10.4236/ampc.2017.77022

Received: June 14, 2017
Accepted: July 22, 2017
Published: July 25, 2017

Abstract

In this study, the effects of Nb substitution on the Bi-based superconducting materials have been investigated. The X-ray diffraction measurement indicated coexistence of Bi-2212, Bi-2223 phases and some impurity phases of CuO, $CuNb_2O_6$, $CaNb_2O_6$, $CaCuO_2$, and $Sr_5Nb_5O_{16}$. With increasing Nb content, impurity phases consistent with the Nb element appeared in the samples. Also with increasing Nb content, the Bi-2223 phase of samples gradually was decreased and in contrast, the Bi-2212 phase was increased. From the SEM, results have been seen that with increasing of Nb contents, the crystal structure of the samples was slightly changed because of the disrupted grain growth. From the electrical resistivity measurements, it has been found that with increasing of Nb contents, critical temperature decreases and the superconducting transition width (ΔT) increases. Estimated critical current density showed that J_c decreases with increasing Nb content, as expected.

Keywords

H-T Superconductors, Bi-2223 Phase, Bi-2212 Phase, Bi-2201 Phase, X-Ray Diffraction

1. Introduction

In high-temperature superconductors, there is a group which is called the Bi-based superconductors. Following the discovery of Bi-based superconductors [1], researchers work on this type of high-temperature superconductors. A lot of works have been done in the field of high-temperature superconductors [2]-[10] in order to improve their critical current density (J_c), critical temperature (T_c),

and better understand the structural properties of Bi-based superconductors. The Bi-based superconductors are defined by the $Bi_2Sr_2Ca_{n-1}Cu_nO_{2n+4+y}$ general formula and with abbreviations of the BSCCO. In this formula, n is determined with values 1, 2 and 3 which indicates the number of CuO_2 layers in the crystal structure of Bi-based superconductors. In general, Bi-based superconductors have three phases Bi-2201, Bi-2212 and Bi-2223 with around 20, 85, and 110 K critical temperatures, respectively [11] [12] [13]. Among these phases, the Bi-2223 phase with the chemical formula of $Bi_2Sr_2Ca_2Cu_3O_{10+y}$ appears to be suitable for superconducting devices which are operating at a temperature of liquid nitrogen ($T > 77$ K) [14]. But the formation of pure Bi-2223 phase is a critical issue in fabricating BSCCO superconductors.

Before, the researchers have studied the effect of the high-valency cations, like Ta^{5+}, V^{5+}, Nb^{5+} and Nd^{3+} for obtaining of Bi-2223 single phase and found that doping any one of them can significantly enhance the formation of Bi-2223 phase. These cation roles are quite similar to Pb for stabilizing the Bi-2223 phase [15] [16] [17]. Double substitution of Pb with other elements is being attempted for further improvement in Bi-based superconductors so that enhances the transition temperature or the critical current density (J_c) [18]. Ekicibil *et al.* studied the effect of Gd concentration on the properties of $Bi_{1.7}Pb_{0.35-x}Gd_xSr_2Ca_3Cu_4O_{12+y}$ superconductors. They found that with increasing of Gd content, the Bi-2223 phase decreases and the insulating phase increases. In the other words, even with very small amount of Gd^{3+} substation, $Pb^{2+} \rightarrow Gd^{3+}$, superconducting properties degrades by decreasing the hole concentration [19].

In this research, our aims are:

1) To answer this question that substitution of Pb with Nb in BPSCCO systems increases or decreases the critical temperature.

2) To explore the magnetic behavior of the modified BPSCCO systems. In other words, this substitution improves or depresses the superconductivity of BPSCCO systems.

Our simple are BPSSCO system with general formula of $Bi_{1.65}Pb_{0.35-x}Nb_xSr_2Ca_2Cu_3O_{10+\delta}$ and x = 0.0, 0.05, 0.15, 0.25, 0.35.

2. Experimental

$Bi_{1.65}Pb_{0.35-x}Nb_xSr_2Ca_2Cu_3O_{10+\delta}$ samples, with x = 0.0, 0.05, 015, 0.25 and 0.35 substitutions were prepared from ultra-fine and high grade purity powders Bi2O3 (99.99%), PbO (99.99%), $SrCO_3$ (99.99%), CaCO3 (99.9%), Nb_2O_5 (99.99%) and CuO (99.99%) using the conventional solid-state reaction method [20]. The starting powders in stoichiometric proportions were weighted and well mixed (the precursors have milled approximately for 1 h) and pressed to pellets by using hydraulic press type. The pellets were first calcined at 810˚C for 48 h in order to start the formation of the superconducting phases. Then the pellets were ground and mixed in an agate mortar pestle, the resulting powder from the calcination process pressed into pellets, and sintered at 825˚C in the air for 48 h.

For the preparation of pellets from powders, dry pressing at 250 MPa in calcination processes and pressing at 450 MPa in the final process were employed. Our samples were disc-shaped pellets with 13 mm diameter and 2 mm thickness. Finally, the pellets (samples) were sintered at 845˚C for 100 h in air and slowly furnace cooled to room temperature. We labeled our samples A (x = 0.00), B (x = 0.05), C (x = 0.15), D (x = 0.25) and E (x = 0.35). The heat treatment schedule for (Bi, Pb)-2223 pellets in programmable temperature controlled furnace is shown in Figure 1.

For measurement of the DC resistivity of samples as a function of temperature, the standard four-point probe method with silver point contacts was used. The transition temperature T_C was determined as the temperature at zero resistivity. The structure of the samples was checked by SIMENS X-ray diffractometer with CuKα (1.54 Å) radiation in the range of $2\theta = 2^\circ$ - 60°. Lattice parameters were determined from the XRD patterns by using Match 3.3 software based on Cohen's least square method. Scanning electron microscope (SEM) photographs for the study of the microstructure were taken by using MIRA3 TESCAN. Magnetic measurements of samples were done by a Quantum Design PPMS model 6000.

3. Results and Discussion

Figure 2 shows the XRD patterns of samples A to E, which Nb was substituted in the form of Nb_20_5. Obtained results from XRD patterns indicated coexistence of the Bi-2212 and Bi-2223 phases and some impurity phases. Impurity phases such as CuO, $CaCuO_2$, $CuNb_2O_6$, $CaNb_2O_6$, and $Sr_5Nb_5O_{15}$ were detected in the

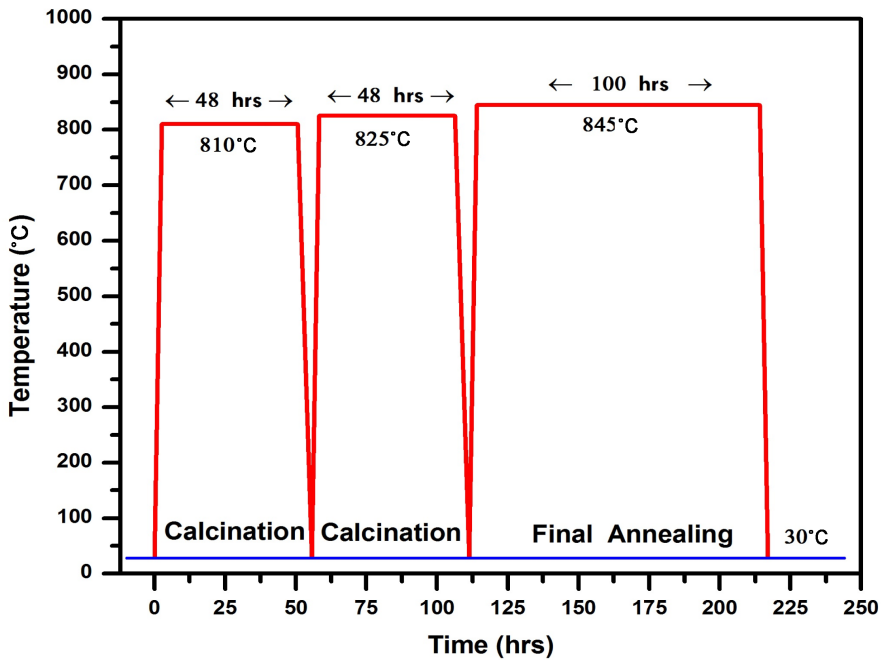

Figure 1. The heat treatment schedule for Bi-2223 programmable temperature controlled furnace.

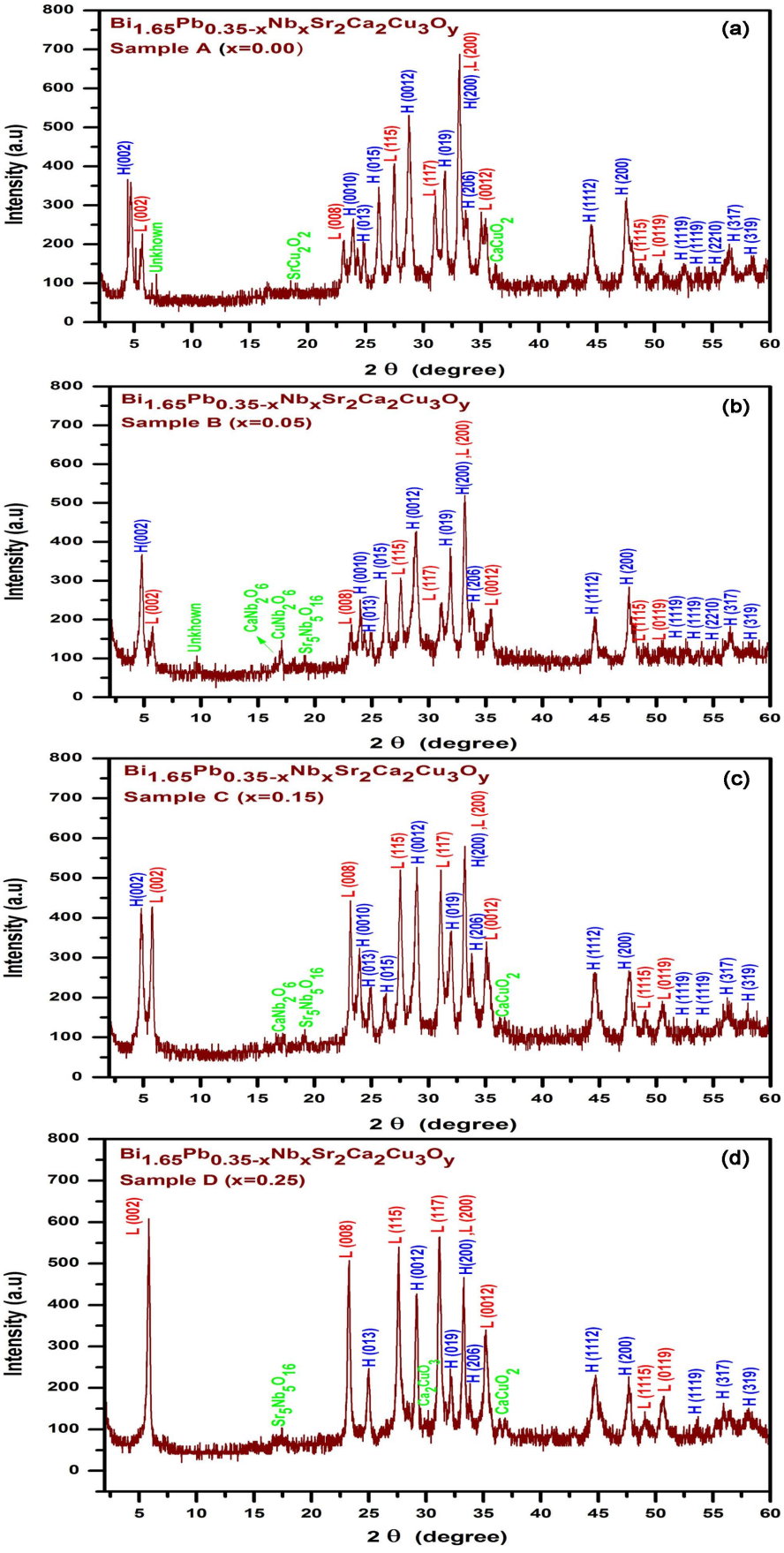
Bi1.65Pb0.35-xNbxSr2Ca2Cu3Oy
Sample A (x=0.00)
(a)
Intensity (a.u)
2 θ (degree)
H(002)
L (002)
Unkhown
SrCu2O2
L (008)
H (0010)
H (013)
H (015)
L (115)
H (0012)
L (117)
H (019)
H(200) ,L (200)
H (206)
L (0012)
CaCuO2
H (1112)
H (200)
L (1115)
L (0119)
H (1119)
H (1119)
H (2210)
H (317)
H (319)
Bi1.65Pb0.35-xNbxSr2Ca2Cu3Oy
Sample B (x=0.05)
(b)
Intensity (a.u)
2 θ (degree)
H(002)
L (002)
Unkhown
CaNb2O6
CuNb2O6
Sr5Nb5O16
L (008)
H (0010)
H (013)
H (015)
L (115)
H (0012)
L (117)
H (019)
H(200) ,L (200)
H (206)
L (0012)
H (1112)
H (200)
L (1115)
L (0119)
H (1119)
H (1119)
H (2210)
H (317)
H (319)
Bi1.65Pb0.35-xNbxSr2Ca2Cu3Oy
Sample C (x=0.15)
(c)
Intensity (a.u)
2 θ (degree)
H(002)
L (002)
CaNb2O6
Sr5Nb5O16
L (008)
H (0010)
H (013)
H (015)
L (115)
H (0012)
L (117)
H (019)
H(200) ,L (200)
H (206)
L (0012)
CaCuO2
H (1112)
H (200)
L (1115)
L (0119)
H (1119)
H (1119)
H (317)
H (319)
Bi1.65Pb0.35-xNbxSr2Ca2Cu3Oy
Sample D (x=0.25)
(d)
Intensity (a.u)
2 θ (degree)
L (002)
Sr5Nb5O16
L (008)
H (013)
L (115)
H (0012)
Ca2CuO3
L (117)
H (019)
H(200) ,L (200)
H (206)
L (0012)
CaCuO2
H (1112)
H (200)
L (1115)
L (0119)
H (1119)
H (317)
H (319)

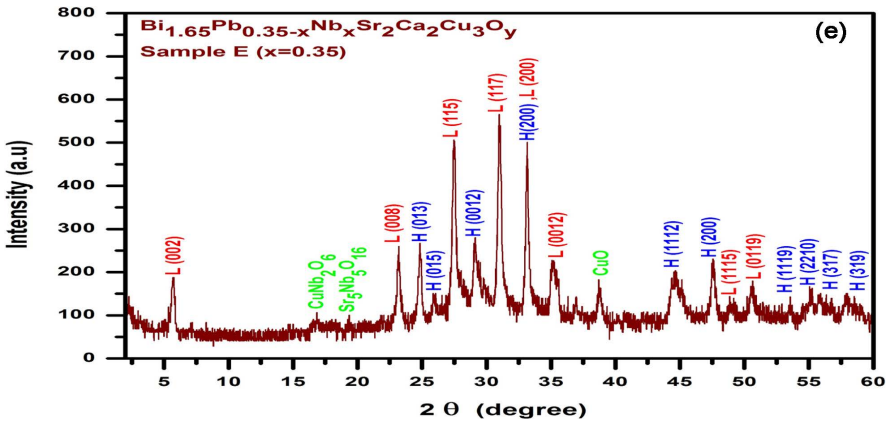

Figure 2. The XRD patterns of the samples A to E.

diffraction angle 2θ range between 2˚ - 60˚. Comparison of five highest peaks and detected impurity phases of samples by using Match 3.3 software are given in Table 1. The intensity of L(002) peak at $2\theta = 5.7^{\circ}$ which is the characteristic peak of Bi-2212 phase, with increasing Nb content up to x = 0.25 increases. Intensity of H(002) peak at $2\theta = 4.7^{\circ}$ which is the characteristic peak of Bi-2223 phase, with increasing Nb content up to x = 0.15 decreases and then in samples D and E disappears. As it can be seen from Figure 2 by increasing of the Nb substitution the impurity phases of the samples increase. This means that, with the substitution of Pb^{2+} ions with Nb^{5+} ions, niobium (with melting point = 1512˚C) is not dissolved completely within the main matrix during heat treatment cycle (845˚C). Niobium participates in the formation of the various impurity phases.

For determining the volume fraction of the present phases of the samples, following equations were used by means of corresponding XRD peaks of Bi-2223 and Bi-2212 phases [21] [22]:

$$\text{Bi-2223}(\%) \approx \frac{\Sigma I(\text{Bi-2223})}{\Sigma I(\text{Bi-2223}) + \Sigma I(\text{Bi-2212})} \times 100 \quad (1)$$

$$\text{Bi-2212}(\%) \approx \frac{\Sigma I(\text{Bi-2212})}{\Sigma I(\text{Bi-2223}) + \Sigma I(\text{Bi-2212})} \times 100 \quad (2)$$

where I(Bi-2223) and I(Bi-2212)) are the intensity of present phases in the samples which were indicated in Figure 2. The percentage volume fraction of the present BSCCO phases of the samples listed in Table 2. As seen in this table, samples A, B, C, D and E contained 63.7%, 64.8%, 56.4%, 46.2%, and 48.7% of the Bi-2223 phase, respectively. Increasing Nb substitution up to x = 0.25 in our samples resulted in an enhancement of the volume fraction of the Bi-2212 phase. The percent amount of the Bi-2223 and Bi-2212 phases as a function of Nb substitution (x) evaluated from the XRD patterns of the A to E samples are given in Figure 3.

Small impurity peaks of samples were identified by using Match 3.3 Software. For example, Figure 4(a) and Figure 4(b) show the match Ritveld refinement

Table 1. Comparison of five highest peaks and impurity phase of $Bi_{1.65}Pb_{0.35-x}Nb_xSr_2Ca_2Cu_3O_{10+\delta}$.

Sample (Nb substation)	Nominal Composition	2θ	d-values	Peak name	(hkl)
		4.73	18.677	Bi-2223	H(002)
		27.5	3.241	Bi-2223	H(115)
		28.80	3.097	Bi-2223	H(117)
A (x = 0.00)	$Bi_{1.65}Pb_{0.35}Sr_2Ca_2Cu_3O_{10+\delta}$	31.87	2.806	Bi-2223	H(119)
		33.13	2.701	Bi-2223	H(200)
		18.56	4.777	$SrCu_2O_2$	I(011)
		36.24	2.477	$CaCuO_2$	I(101)
		4.80	18.382	Bi-2223	H(002)
		26.25	3.392	Bi-2223	H(115)
		28.86	3.091	Bi-2223	H(117)
		31.91	2.870	Bi-2223	H(119)
B (x = 0.05)	$Bi_{1.65}Pb_{0.3}Nb_{0.05}Sr_2Ca_2Cu_3O_{10+\delta}$	33.80	2.696	Bi-2223	H(200)
		16.50	5.367	$CaNb_2O_6$	I(110)
		17.05	5.197	$CuNb_2O_6$	I(110)
		19.12	4.637	Sr_5Nb5O_{16}	I(070)
		5.76	15.336	Bi-2212	L(002)
		23.95	3.712	Bi-2212	L(008)
		27.56	3.234	Bi-2212	L(115)
		28.97	3.079	Bi-2223	H(0012)
C (x = 0.15)	$Bi_{1.65}Pb_{0.2}Nb_{0.15}Sr_2Ca_2Cu_3O_{10+\delta}$	33.19	2.697	Bi-2212	H(200)
		16.72	5.305	$CaNb_2O_6$	I(110)
		19.10	4.643	$Sr_5Nb_5O_{16}$	I(070)
		36.31	2.472	$CaCuO_2$	I(101)
		5.83	15.137	Bi-2212	L(002)
		23.28	3.818	Bi-2212	L(008)
		27.61	3.228	Bi-2212	L(115)
		29.18	3.058	Bi-2223	H(0010)
D (x = 0.25)	$Bi_{1.65}Pb_{0.1}Nb_{0.25}Sr_2Ca_2Cu_3O_{10+\delta}$	31.17	2.867	Bi-2212	L(117)
		17.42	5.087	$Sr_5Nb_5O_{16}$	L(031)
		28.41	3.138	Ca_2CuO_3	I(101)
		36.43	2.464	CaCuO2	I(101)
		23.20	3.830	Bi-2212	L(008)
		24.86	3.579	Bi-2212	H(013)
		27.49	3.241	Bi-2212	L(115)
		31.03	2.879	Bi-2212	L(117)
E (x = 0.35)	$Bi_{1.65}Nb_{0.35}Sr_2Ca_2Cu_3O_{10+\delta}$	33.16	2.699	Bi-2223	H(200)
		17.02	5.213	$CuNb_2O_6$	I(110)
		19.11	4.639	$Sr5Nb_5O_{16}$	I(070)
		38.82	2.318	CuO	I(200)

Table 2. Percentage volume fraction of Bi-2223 and Bi-2212 phases in the samples.

Volume fraction of phases (%)			
Sample (Nb content)	Nominal Composition	Bi-2223 (%)	Bi-2212 (%)
A (x = 0.00)	$Bi_{1.65}Pb_{0.35}Sr_2Ca_2Cu_3O_{10+\delta}$	63.7	36.3
B (x = 0.05)	$Bi_{1.65}Pb_{0.3}Nb_{0.05}Sr_2Ca_2Cu_3O_{10+\delta}$	64.8	35.2
C (x = 0.15)	$Bi_{1.65}Pb_{0.2}Nb_{0.15}Sr_2Ca_2Cu_3O_{10+\delta}$	56.4	43.6
D (x = 0.25)	$Bi_{1.65}Pb_{0.1}Nb_{0.25}Sr_2Ca_2Cu_3O_{10+\delta}$	46.2	53.8
E (x = 0.35)	$Bi_{1.65}Nb_{0.35}Sr_2Ca_2Cu_3O_{10+\delta}$	48.7	51.3

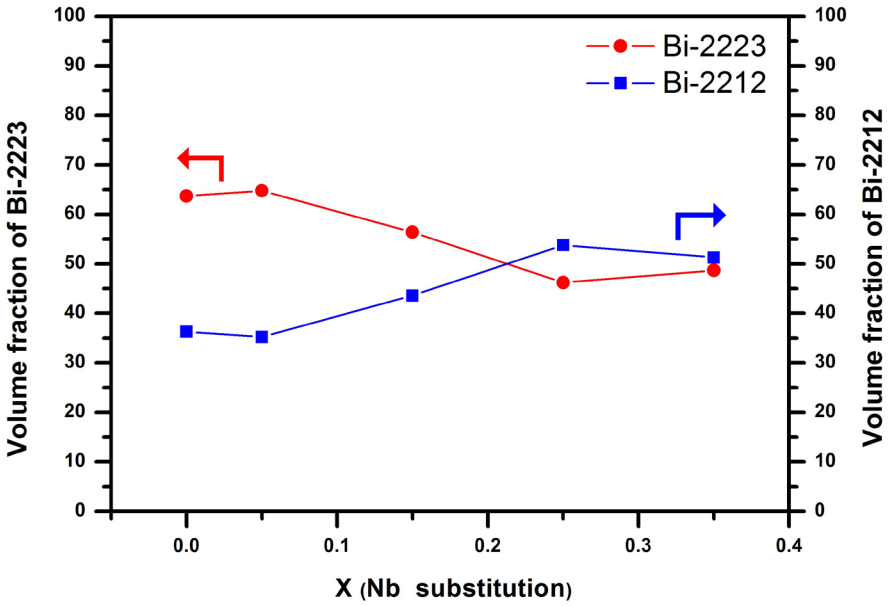

Figure 3. Volume fraction of Bi-2223 and Bi-2212 phases' as a function of Nb substitution.

and impurity phases of the A and E samples [23] [24] [25].

Many properties of the polycrystalline materials depend on the grains size. So, by using of the Debye-Scherer formula in Match 3.3 software and the XRD data, grains size were calculated [26].

$$L_{hkl} = \frac{0.9\lambda}{\beta \cos\theta} \tag{3}$$

where β is the full width at half maximum of X-ray peaks (radians), λ is the wavelength of the incident radiation, and θ is the angle of the peak. With using Debye-Scherer formula, the size of the grains calculated lies between 250 Å and 360 Å.

With calculation of crystal lattice parameters by using Match 3.3 software, were found that all of the samples have an orthorhombic structure which has been reported also by other groups [27] [28]. As seen in **Table 3**, with increasing Nb substitution, c-parameter decreases simultaneously, but in a and b-parameters there are not regular changes. These changes in the parameter of c correlate with decreasing holes concentration in the CuO_2 plane, as suggested by

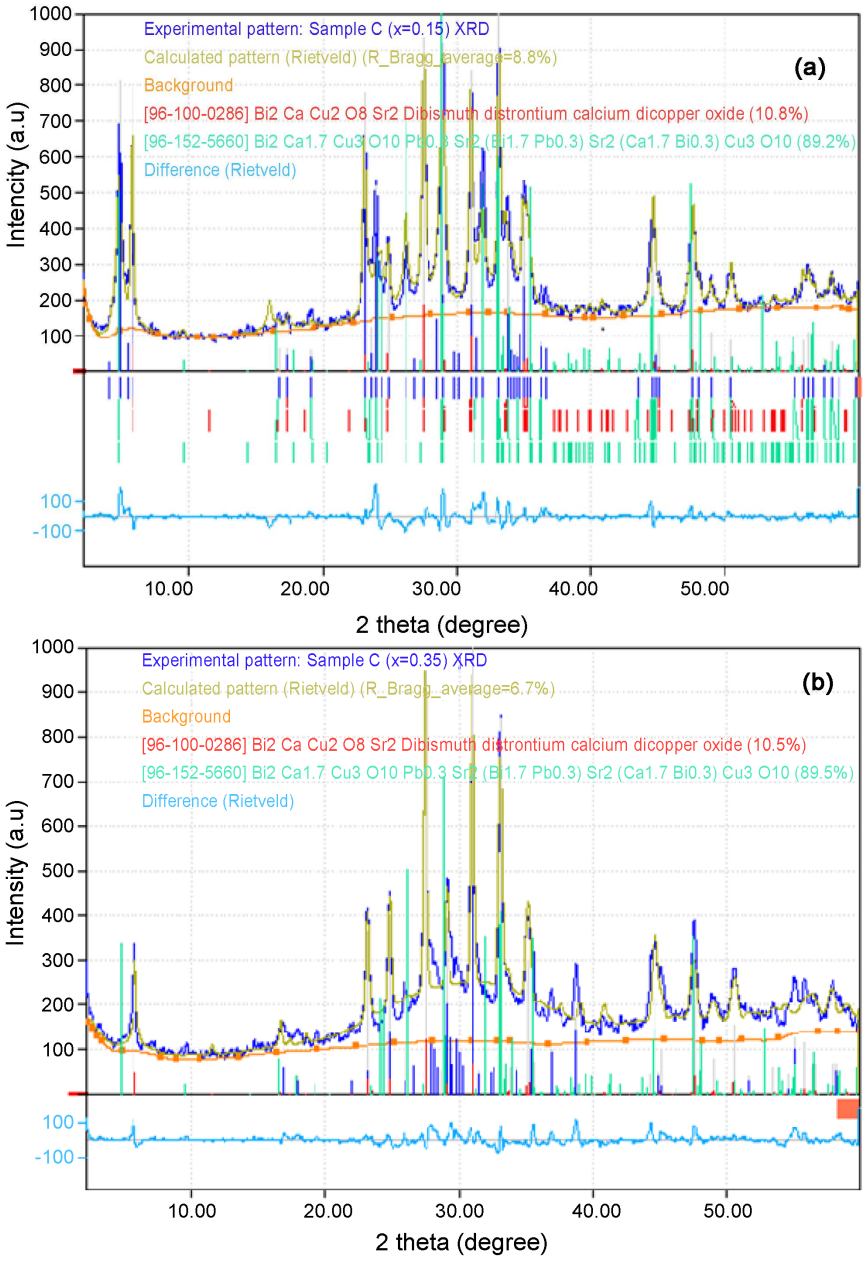

Figure 4. Match ritveld refinement of the C and E samples.

Table 3. Percentage summary of critical temperature T_c^{offset} $(R = 0)$, T_c^{onset}, transition width (ΔT_c), cell parameters of the Bi-2223 phase and *P*-values for different Nb substitution.

Sample (Nb substation)	T_c^{offset} (K)	T_c^{onset} (K)	ΔT_c (K)	*a* (Å)	*b* (Å)	*c* (Å)	*P*-values
A (x = 0.00)	95.1	111.4	16.3	5.40038	5.40882	37.12406	0.120
B (x = 0.05)	91.7	109.3	17.6	5.40546	5.40534	37.10640	0.115
C (x = 0.15)	74.9	112.2	37.3	5.24895	5.59561	37.05370	0.098
D (x = 0.25)	51.4	109.1	57.7	5.40020	5.40112	36.96917	0.080
E (x = 0.35)	50.3	107.9	57.6	5.40031	5.41910	36.95215	0.079

Satyavathi *et al.* and Zandbergen *et al.* [29] [30]. If the valance states of the Bi and Nb are supposed to be unchanged in the material (Bi^{3+} and Nb^{5+}), since the ionic radius of Nb^{5+} (0.7 Å) is different from Bi^{3+} (0.96 Å), probably this is a reason for changing of the unit cell parameters.

Normalized resistivity versus temperature for all samples and the variation of T_c^{offset} with Nb content (x), is given in **Figure 5**. All samples exhibit metallic behavior, this means that resistivity decreases with decreasing temperature. **Table 3** summarize the value of critical temperature T_c^{offset}, T_c^{onset} and transition width $\Delta T_c = T_c^{\text{offset}} - T_c^{\text{onset}}$ for all samples. Samples A and E have the maximum and minimum critical temperature T_c^{offset} (R = 0) with the amount of 95.1 K and 50.3 K respectively. The T_c^{offset} is further decreased in the samples D and E. This result may be due to a decrease of the Bi-2223 phase and increasing of the Bi-2212 phase and especially increasing impurity phases in these samples as extracted from XRD result analysis.

A sharp drop of resistivity was seen for samples A (x = 0.00) and B (x = 0.05), this means that these samples consist of predominantly of Bi-2223 phase. As was indicated by Bolat *et al.*, once the volume fraction of Bi-2223 within the sample is sufficient to make this possible that a one-step resistivity transition is observed even in the samples which contain a rather large amount of Bi-2223 phase [31]. Samples with x = 0.15, 0.25 and 0.35 showed long tail (a high transition width), the reason may existence of the small amount of the Bi-2212 phase and impurity phases or non-superconducting regions or multi superconducting phases in the samples.

Sample with x = 0.25 showed the two-step resistivity transition. It is possible that the both Bi-2223 and Bi-2212 phases exist within one grain in such a way that low-T_c (Bi-2212) phase can play important role in the weak link [27].

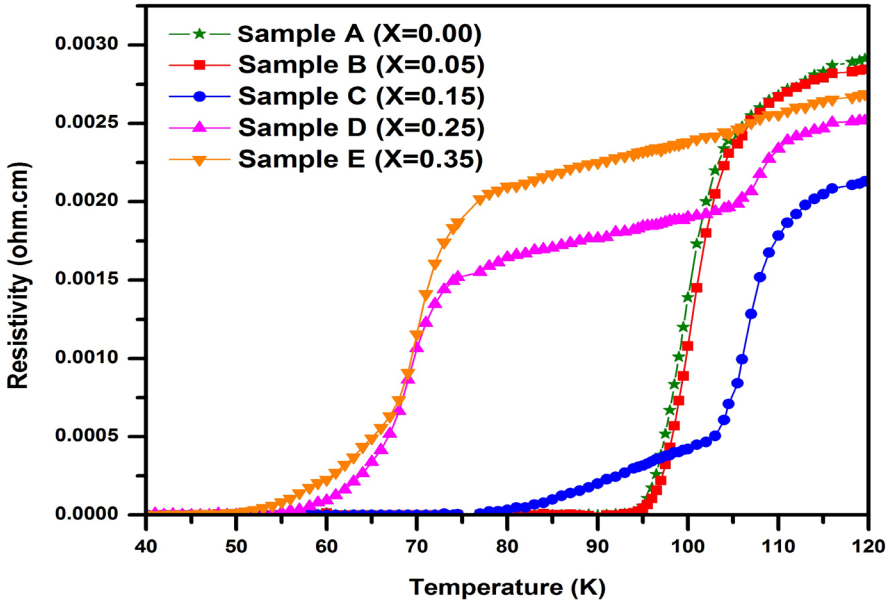

Figure 5. Electrical resistivity versus temperature curves for all samples between 40 and 120.

The zero field cooled (ZFC) magnetization versus temperature curve of samples were measured under external applied magnetic field of 50 Oe. These results are illustrated in Figure 6. The diamagnetic behavior of the samples below their onset temperatures is seen from M-T curves. Additionally, from M-T curves it can be concluded that samples A (x = 0.00) and E (x = 0.35) show the maximum and minimum diamagnetic property among the samples and a reducing tendency on the superconducting properties with the increasing of Nb content.

For determining the intergranular critical current density, the magnetic-hysteresis cycles were measured at 10 K for all samples between applied fields of ±9000 Oe. These results are shown in Figure 7. The obtained results for M-H curves like the M-T curves prove that the sample A with no substitution of Nb is a much better superconductor than the others. By using Bean's critical state model, critical current density (J_c) of samples were calculated from the hysteresis loops [32]. In Bean's critical state model, critical current density proportional to the width of hysteresis loop $\Delta M = \left|M_+ - M_-\right|$ and calculates with this formula:

$$J_c = 20\frac{\left|\Delta M\right|}{a\left(1-\frac{b}{3a}\right)} \tag{4}$$

In this formula, J_c is the critical current density in amperes per square centimeter of a sample and M_+ and M_- magnetizations are obtained from the intersections of M-H loops. ΔM is measured in electromagnetic units per cubic centimeter. Where a and b $(a > b)$ are the sample dimensions perpendicular to the applied field. Critical current density (J_c) versus applied magnetic field

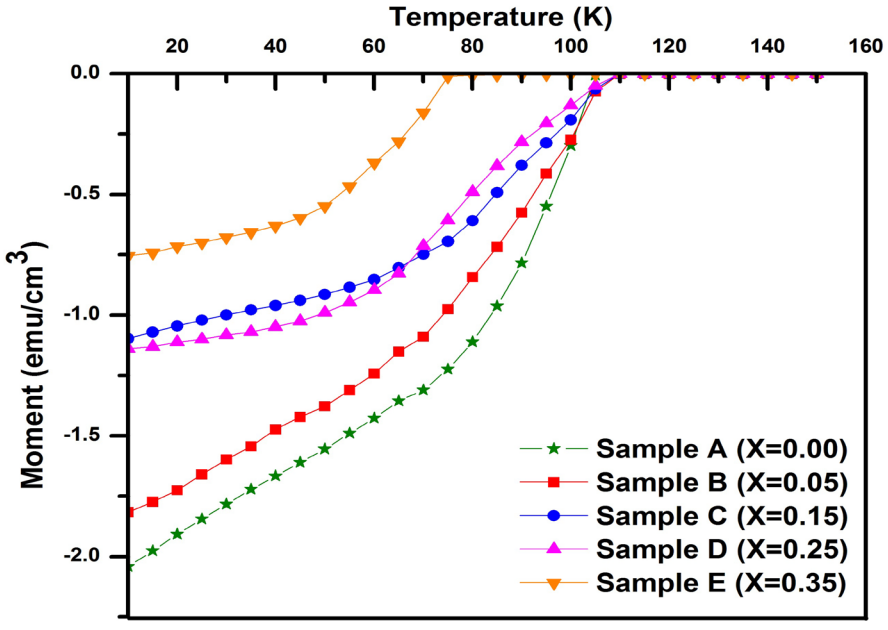

Figure 6. Magnetization versus temperature curves for all samples with an applied field of 50 Oe.

curves are illustrated in Figure 8. The critical current density of samples are 4.60 × 10^3 A·cm^{-2}, 4.48 × 10^3 A·cm^{-2}, 3.99 × 10^3 A·cm^{-2}, 3.53 × 10^3 A·cm^{-2} and 1.53 × 10^3 A·cm^{-2} for the samples A, B, C, D and E respectively. As can be seen from Figure 8, the sample A with no substitution of Nb, has larger critical current density than those of the others. With increasing of Nb content in our samples, critical current density decreases. Our results show that Pb^{2+} substitution by Nb^{5+} degrades the superconducting properties of the samples.

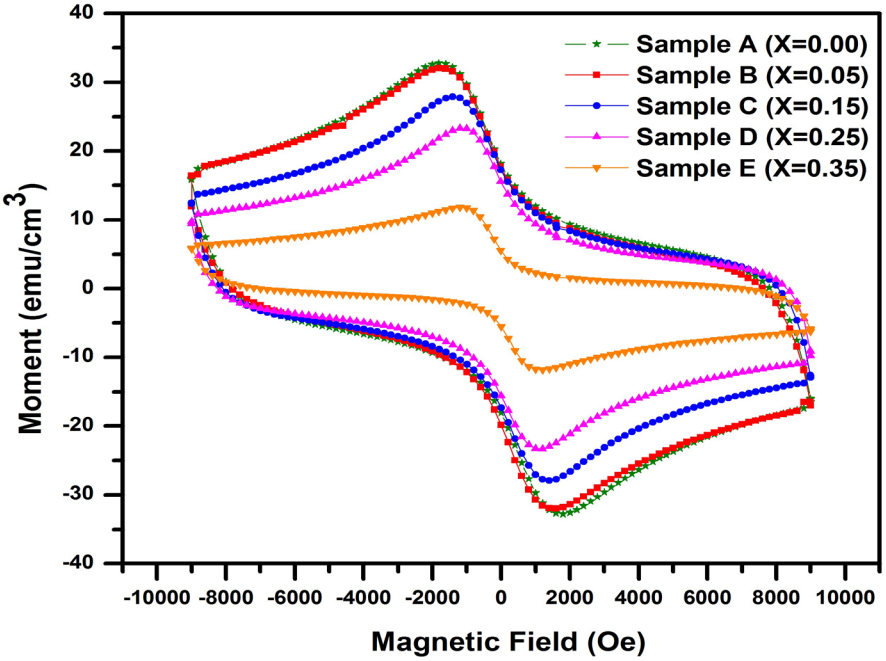

Figure 7. M-H hysteresis curves for all samples at temperature of 10 K.

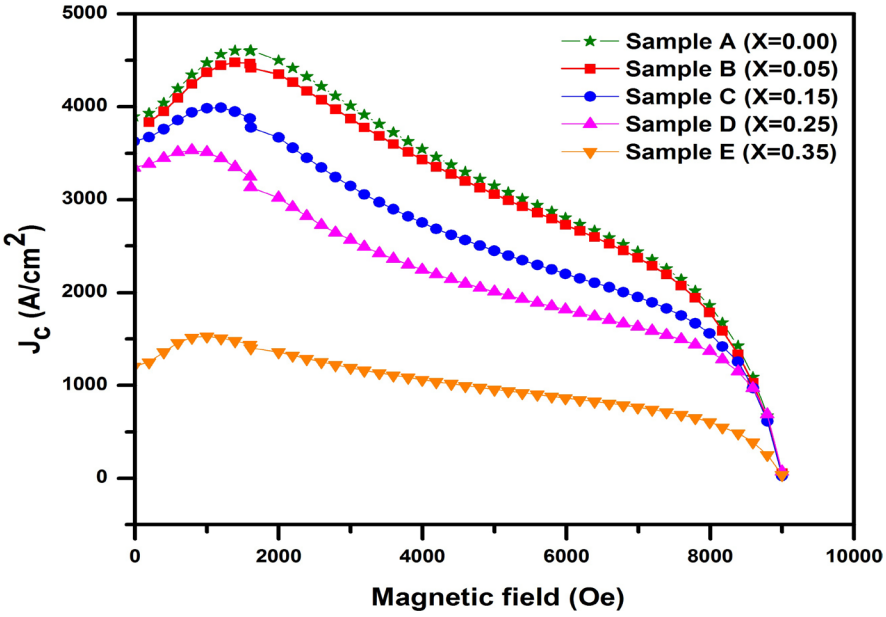

Figure 8. Critical current density (J_c) of $Bi_{1.65}Pb_{0.35-x}Nb_xSr_2Ca_2Cu_3O_{10+\delta}$ (x = 0.0, 0.05, 0.15, 0.25, 0.35) at 10 K.

In ceramic high-temperature superconductors, one of the most important properties is their grain structure. These grain structures can be illustrated and explained by the SEM micrographs. These SEM micrographs provide us with data about the formation of the surface morphology of the samples. Surface morphology micrographs taken by SEM for all samples are shown in **Figure 9**. Other researchers indicated that morphology of BSCCO systems composed of randomly plate-like grains with unfilled spaces between them [33] [34]. SEM micrographs indicated that the grain size and the distribution of grains on the surfaces of the samples are quite different. The structure of sample A with no Nb^{5+} has large plate-like grains, which is characteristic of the grain structure of Bi-2223 phase. In contrast, SEM micrograph of sample E with no Pb^{2+} contains the mixture of different sized flaky and plate-like grains which are connected with each other while there are some unfilled spaces among them as expected for Bi-2212 phase. Consistent with XRD results, substitution of Nb^{5+} ions with Pb^{2+}, the Bi-2223 phase has gradually transformed into the Bi-2212.

Superconducting transition temperature has a parabolic relationship with the hole concentration p (the number of holes per Cu atom) can be calculated by using this relation which is given by Presland *et al.* [35].

$$\frac{T_c}{T_c^{\max}} = 1 - 82.6\left(p - 0.16\right)^2 \tag{5}$$

In this formula for the Bi-2223 and Bi-2212 systems the value of $T_c^{\max}$ is taken 110 K and 85 K respectively and T_c^{offset} values are taken from **Table 2**. Recently, this formula was successfully applied to Bi-based superconducting systems [36] [37]. Superconductivity researchers in the previous calculations for the unsubstituted Bi-2223 system have shown that the values of p ranged from 0.116 to 0.160. In this study, p-values of the A, B, C, D, and E samples have calculated 0.119, 0.115, 0.098, 0.080 and 0.079, respectively. The results obtained, show that the p-values of our samples seem to decrease slightly with increasing Nb concentration. Therefore, the increase in the normal-state resistivity value of the samples (ρ at T_c^{onset}) can be attributed to hole filling mechanism that presented by Gondogmuş *et al.* [38]. Based on the obtained results, sample A has the best electrical characteristic among the samples and with increasing Nb content,

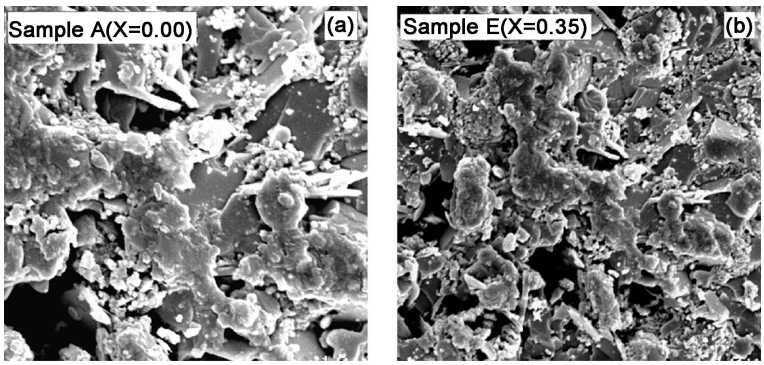

Figure 9. SEM micrograph for samples A and E.

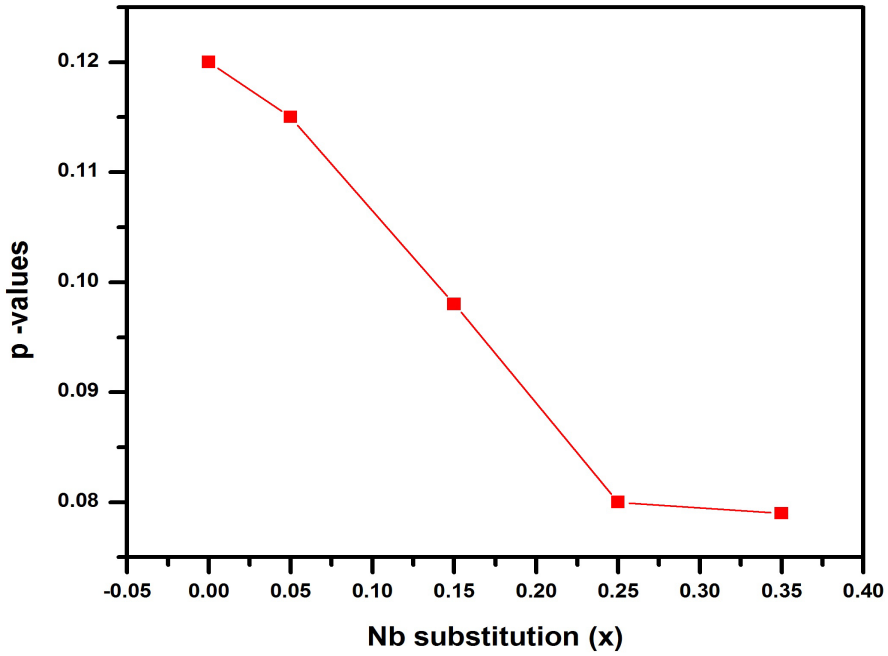

Figure 10. *P*-values versus Nb substitution in $Bi_{1.65}Pb_{0.35-x}Nb_xSr_2Ca_2Cu_3O_{10+\delta}$ (x = 0.00, 0.05, 0.15, 0.25, 0.35).

superconducting properties degrade. *p*-values versus Nb substitution is shown in Figure 10.

4. Conclusion

In summary, the nominal composition of the $Bi_{1.65}Pb_{0.35-x}Nb_xSr_2Ca_2Cu_3O_{10+\delta}$ (x = 0.0, 0.05, 0.15, 0.25 and 0.35) compounds has been prepared by the solid-state reaction method and the effects of Pb^{2+} substitution by Nb^{5+} in (Bi-Pb)-2223 superconducting samples have been investigated. The obtained results from XRD, resistance measurements, DC magnetization and hysteresis measurements showed that with increasing of Nb content volume fraction of the high-T_c (Bi-2223) phase, the critical temperature $\left(T_c^{\text{offset}}\right)$ and critical current density (J_c) of the samples decreased. In the other words, Pb^{2+} substitution by Nb^{5+} degrades the superconducting properties of the samples. In the sintering temperature range of 840˚C - 860˚C, two phases of Bi-2212 and Bi-2223 are formed. For the high-T_c (Bi-2223) phase formation and large growth of grain size, sintering temperature must be close to the partial melting point of composing elements of BSCCO system. The melting point of Nb_2O_5 (1512˚C) is much higher than the sintering temperature of BSCCO system and a melting point of PbO (888˚C). For this reason, with increasing of Nb content impurity phases of samples, Pb substitution with Nb in BPSCCO system decreases superconducting properties.

Acknowledgements

The authors would like to thank Superconductivity Research Center of Urmia University and Gebze Technical University for supporting and helping us with

the all the related measurements of this project. The authors would also like to express their thanks to Professor Ali Gerncer, Center of Excellence for Superconductivity Research, Ankara University, Turkey for helpful discussions.

References

[1] Maeda, H., Tanaka, Y. Fukutomi, M. and Asano, T. (1988) A New High-T_c Oxide Superconductor without a Rare Earth Element. *Japanese Journal of Applied Physics*, **27**, L209. http://iopscience.iop.org/article/10.1143/JJAP.27.L209 https://doi.org/10.1143/JJAP.27.L209

[2] Ozçelik, B., Gundogmuş, H. and Yazıcı, D. (2014) Effect of (Ta/Nb) Co-Doping on the Magneto Resistivity and Flux Pinning Energy of the BPSCCO Superconductors. *Journal of Materials Science*: *Materials in Electronics*, **25**, 2456-2462. https://link.springer.com/article/10.1007/s10854-014-1895-1 https://doi.org/10.1007/s10854-014-1895-1

[3] Ozçelik, B., Kaya, C., Gundogmuş, H., Sotelo, A. and Madre, M.A. (2014) Effect of Ce Substitution on the Magneto resistivity and Flux Pinning Energy of the $Bi_2Sr_2Ca_{1-x}Ce_xCu_2O_{8+\delta}$ Superconductors. *Journal of Low Temperature Physics,* **174**, 136-147. https://link.springer.com/article/10.1007/s10909-013-0954-y https://doi.org/10.1007/s10909-013-0954-y

[4] Turk, N., Gundogmuş, H., Akyol, M., Yakıncı, Z.D., Ekicibil, A. and Ozçelik, B. (2014) Effect of Tungsten (W) Substitution on the Physical Properties of Bi-(2223) Superconductors. *Journal of Superconductivity and Novel Magnetism,* **27**, 711-716. https://link.springer.com/article/10.1007/s10948-013-2351-9 https://doi.org/10.1007/s10948-013-2351-9

[5] Ozaslan, A., Ozçelik, B., Ozkurt, B., Sotelo, A. and Madre, M.A. (2014) Structural, Electrical, and Magnetic Properties of the Co-Substituted Bi-2212 System Textured by Laser Floating Zone Technique. *Journal of Superconductivity and Novel Magnetism,* **27**, 53. https://link.springer.com/article/10.1007/s10948-013-2257-6 https://doi.org/10.1007/s10948-013-2257-6

[6] Gundogmuş, H., Ozçelik, B., Sotelo, A. and Madre, M.A. (2013) Effect of Yb-Substitution on Thermally Activated Flux Creep in the $Bi_2Sr_2Ca_1Cu_{2-x}Yb_xO_y$ Superconductors. *Journal of Materials Science*: *Materials in Electronics*, **24**, 2568-2575. https://link.springer.com/article/10.1007/s10854-013-1135-0 https://doi.org/10.1007/s10854-013-1135-0

[7] Ozçelik, B., Ozkurt, B., Yakıncı, M.E., Sotelo, A. and Madre, M.A. (2013) Relationship between Annealing Time and Magnetic Properties in Bi-2212 Textured Composites. *Journal of Superconductivity and Novel Magnetism,* **26**, 873-878. https://link.springer.com/article/10.1007/s10948-012-1874-9 https://doi.org/10.1007/s10948-012-1874-9

[8] Yazıcı, D., Ozçelik, B. and Yakıncı, M.E. (2011) Improvement of High Tc Phase Formation in BPSCCO Superconductor by Adding Vanadium and Substituting Titanium. *Journal of Low Temperature Physics,* **163**, 370-379. https://link.springer.com/article/10.1007/s10909-011-0355-z https://doi.org/10.1007/s10909-011-0355-z

[9] Abou-Aly, A.I., Abdel Gawad, M.M.H., Awad, R. and G-Eldeen, I. (2011) Improving the Physical Properties of (Bi, Pb)-2223 Phase by SnO_2 Nano-Particles Addition. *Journal of Superconductivity and Novel Magnetism,* **24**, 2077. https://link.springer.com/article/10.1007/s10948-011-1171-z https://doi.org/10.1007/s10948-011-1171-z

[10] Abbasi, H., Taghipour, J. and Sedghi, H. (2009) The effect of $MgCO_3$ Addition on the Superconducting Properties of Bi2223 Superconductors. *Journal of Alloys and Compounds*, **482**, 552-555. http://www.sciencedirect.com/science/article/pii/S0925838809007944

[11] Gao, L., Huang, Z.J., Meng, R.L., Hor, P.H., Bechtold, J., Sun, Y.Y., Chu, C.W., Sheng, Z.Z. and Herman, A.M. (1988) Bulk Superconductivity in $Tl_2CaBa_2Cu_2O_{8+\delta}$ up to 120 K. *Nature*, **332**, 623-624. https://doi.org/10.1038/332623a0 https://www.nature.com/nature/journal/v332/n6165/abs/332623a0.html

[12] Chu, C.W., Bechtold, J., Gao, L., Hor, P.H., Huang, Z.J., Meng, R.L., Sun, Y.Y., Wang, Y.Q. and Zue, Y.Y. (1988) Superconductivity up to 114 K in the Bi-Al-Ca-Sr-Cu-O Compound System without Rare-Earth Elements. *Physical Review Letters*, **60**, 941. https://journals.aps.org/prl/abstract/10.1103/PhysRevLett.60.941 https://doi.org/10.1103/physrevlett.60.941

[13] Tallon, L.J., Buckley, R.G., Gilberd, P.W., Presland, M.R., Brown, I.W.M., Bowden, M.E., Christian, L.A. and Goguel, R. (1988) High-T_c Superconducting Phases in the Series $Bi_{2.1}(Ca, Sr)_{n+1}Cu_nO_{2n+4+\delta}$. *Nature*, **333**, 153-156. https://doi.org/10.1038/333153a0 https://www.nature.com/nature/journal/v333/n6169/pdf/333153a0.html

[14] Sozeri, H., Ghazanfari, N., Ozkan, H. and Kılıç, A. (2007) Enhancement in the High-T_c Phase of BSCCO Superconductors by Nb Addition. *Superconductor Science and Technology*, **20**, 522-528. https://doi.org/10.1088/0953-2048/20/6/007 http://iopscience.iop.org/article/10.1088/0953-2048/20/6/007

[15] Yazici, D., Ozçelik, B., Altin, S. and Yakinci, M.E. (2011) Effect of Vanadium-Titanium Co-Doping on the BPSCCO Superconductor. *Journal of Superconductivity and Novel Magnetism*, **24**, 217-222. https://doi.org/10.1007/s10948-010-0921-7 https://link.springer.com/article/10.1007/s10948-010-0921-7

[16] Sykorova, D., Smrckova, O. and Vasek, P. (2000) Chemical Stability of the Bi (Pb)-Sr-Ca-Cu-O Superconductors. *Journal of Superconductivity and Novel Magnetism*, **13**, 899-901. https://link.springer.com/article/10.1023/A:1026429603418

[17] Ozkurt, B., Ekicibil, A., Ali Aksan, M., Ozçelık, B., Yakıncı E.M. and Kiymac, K. (2007) Structural and Physical Properties of Nd Substituted Bismuth Cuprates $Bi_{1.7}Pb_{0.3-x}Nd_xSr_2Ca_3Cu_4O_{12+y}$. *Journal of Low Temperature Physics*, **149**, 105-118. https://doi.org/10.1007/s10909-007-9500-0 https://link.springer.com/article/10.1007/s10909-007-9500-0

[18] Xin, Y., Sheng, Z.Z. and Nasrazadani, S. (1991) Comparison of Pb, Pb&Sb, Pb&V, Pb&Mo and Pb&W substituted $Bi_2Sr_2Ca_2Cu_3O_x$. *Physica C: Superconductivity and Its Applications*, **176**, 179-188. https://doi.org/10.1016/0921-4534(91)90711-7 http://www.sciencedirect.com/science/article/pii/0921453491907117

[19] Ekicibil, A., Coşkun, A., Ozçelik, B. and Kiymac, K. (2005) The Effect of Gd Concentration on the Physical and Magnetic Properties of $Bi_{1.7}Pb_{0.3-x}Gd_xSr_2Ca_3Cu_4O_{12+y}$ Superconductors. *Journal of Low Temperature Physics*, **140**, 105-117. https://doi.org/10.1007/s10909-005-6015-4 https://link.springer.com/article/10.1007/s10909-005-6015-4

[20] Ismail, M., Abd-Shukor, R., Hamadneh, I. and Halim, S.A. (2004) Transport Current Density of Ag-Sheathed Superconductor Tapes Using Bi-Sr-Ca-Cu-O Powders Prepared by the Co-Precipitation Method. *Journal of Materials Science*, **39**, 3517-3519. https://link.springer.com/article/10.1023/B%3AJMSC.0000026965.20428.cb https://doi.org/10.1023/B:JMSC.0000026965.20428.cb

[21] Chiu, C.L., Gao, C.F., Huang, Z.J., Meng, R. and Xue, Y.Y. (1993) Superconductivity above 150 K in $HgBa_2Ca_2Cu_3O_{8+\delta}$ at High Pressures. *Nature*, **365**, 323-325. https://www.nature.com/nature/journal/v365/n6444/abs/365323a0.html https://doi.org/10.1038/365323a0

[22] Driessche, I.V., Buekenhoudt, A., Konstantinov, K., Brueneel, E. and Hoste, S. (1996) Evaluation of the Phase Composition of BPSCCO Bulk Samples by XRD- and Susceptibility Analysis. *Applied Superconductivity*, **4**, 185-190. http://www.sciencedirect.com/science/article/pii/S0964180796000257

[23] Asbrink, S. and Waskowska, A. (1991) CuO: X-Ray Single-Crystal Structure Determination at 196 K and Room Temperature. *Journal of Physics*: *Condensed Matter,* **3**, 8173-8180. http://iopscience.iop.org/article/10.1088/0953-8984/3/42/012/meta https://doi.org/10.1088/0953-8984/3/42/012

[24] Cummings, J.P. and Simonsen, S.H. (1970) The Crystal Structure of Calcium Niobate ($CaNb_2O_6$). *American Mineralogist,* **55**, 90-97. http://www.minsocam.org/msa/collectors_corner/amtoc/toc1970.htm

[25] Norwig, J., Weitzel, H., Paulus, H., Lautenschlaeger, G., Rodriguez-Carvajal, J. and Fuess, H. (1995*)* Structural Relations in Mixed Oxides $Cu_xZn_{1-x}Nb_2O_6$. *Journal of Solid State Chemistry*, **115**, 476-483. http://www.sciencedirect.com/science/article/pii/S0022459685711620 https://doi.org/10.1006/jssc.1995.1162

[26] Cullity, B.D. (1978) Element of X-Ray Diffraction. Addison-Wesley Reading, Boston. https://archive.org/details/elementsofxraydi030864mbp

[27] Abbas, M.M., Oboudi, S.F. and Raoof, N.Q. (2015) Investigating the Preparation Conditions on Superconducting Properties of Bi_{2-x} $Li_xPb_{0.3}Sr_2Ca_2Cu_3O_{10+\delta}$. *Materials Sciences and Applications*, **6**, 310-321. https://doi.org/10.4236/msa.2015.64036 http://www.scirp.org/journal/PaperInforCitation.aspx?PaperID=55420

[28] Ozçelic, B., Gursul, M., Sotelo, A. and Madre, M.A. (2015) Improvement of Superconducting Properties in Na-Doped BSCCO Superconductor. *Journal of Materials Science*: *Materials in Electronics*, **26**, 441-447. https://doi.org/10.1007/s10854-014-2419-8 https://link.springer.com/article/10.1007/s10854-014-2419-8

[29] Satyavathi, S., Kishore, K.N., Babu, V.H. and Pena, O. (1996) Systematics of the Physical Properties of Compounds. *Superconductor Science and Technology*, **9**, 93. http://iopscience.iop.org/article/10.1088/0953-2048/9/2/005/meta https://doi.org/10.1088/0953-2048/9/2/005

[30] Zandbergen, H.W., Groen, W.A., Smit, A. and Van Tendeloo, G. (1990) Structure and Properties of $(Bi, Pb)_2Sr_2(Ca, Y)Cu_2O_{8+\delta}$. *Physica C*: *Superconductivity and Its Applications*, **168**, 426. http://www.sciencedirect.com/science/article/pii/092145349090538P https://doi.org/10.1016/0921-4534(90)90538-P

[31] Bolat, S., Yanmaz, E. and Comert, H. (2000) Properties of Ag-Doped Bi_{(1.6)} Pb_{(0.4)}Sr_2Ca_3Cu_{(4-x)}Ag_xO_y (2234) Oxides Prepared by S.S.R. Method. *Turkish Journal of Physics,* **24**, 129-135. http://journals.tubitak.gov.tr/physics/abstract.htm?id=3897

[32] Bean, C.P. (1962) Magnetization of Hard Superconductors. *Physical Review Letters*, **8**, 250. https://journals.aps.org/prl/abstract/10.1103/PhysRevLett.8.250 https://doi.org/10.1103/physrevlett.8.250

[33] Ozkurt, B. (2013) The Influence of WO_3 Nano-Particle Addition on the Structural and Mechanical Properties of $Bi_{1.8}Sr_2Ca_{1.1}Cu_{2.1}O_y$ Ceramics. *Journal of Materials*

Science, **24**, 4233-4239. https://link.springer.com/article/10.1007/s10854-013-1390-0

[34] Lennikov, V., Ozkurt, B., Angurel, L.A., Sotelo, A., Ozçelik, B. and Fuente, G.F. (2013) Microstructure and Transport Properties of Bi_{-2212} Prepared by CO_2 Laser Line Scanning. *Journal of Superconductivity and Novel Magnetism*, **26**, 947-952. https://link.springer.com/article/10.1007/s10948-012-1934-1 https://doi.org/10.1007/s10948-012-1934-1

[35] Presland, M.R., Tallon, J.L., Buckley, R.G., Liu, R.S. and Floer, N.E. (1991) General Trends in Oxygen Stoichiometry Effects on T_c in Bi and Tl Superconductors. *Physica C: Superconductivity and Its Applications*, **176**, 95-105. http://www.sciencedirect.com/science/article/pii/0921453491907009 https://doi.org/10.1016/0921-4534(91)90700-9

[36] Obertelli, S.D., Cooper, J.R. and Tallon. J.L. (1992) Systematics in the Thermoelectric Power of High-T_c Oxides. *Physical Review B*, **46**, 14928. https://journals.aps.org/prb/abstract/10.1103/PhysRevB.46.14928 https://doi.org/10.1103/PhysRevB.46.14928

[37] Aksan, M.A. and Yakinci, M.E. (2007) Effect of Mo Substitution on the Structural and Transport Properties of $Bi_2Sr_2Ca_2Cu_{3-x}Mo_xO_{10+y}$ System. *Journal of Alloys and Compounds*, **433**, 22-32. http://www.sciencedirect.com/science/article/pii/S0925838806007833?via%3Dihub https://doi.org/10.1016/j.jallcom.2006.06.060

[38] Türk, N., Gondogmuş, H., Akyol, M., Yakinci, Z.D., Ekicibil, A. and Özçelik, B. (2014) Effect of Tungsten (W) Substitution on the Physical Properties of $Bi_{-(2223)}$ Superconductors. *Journal of Superconductivity and Novel Magnetism*, **27**, 711-716. https://link.springer.com/article/10.1007/s10948-013-2351-9 https://doi.org/10.1007/s10948-013-2351-9